Plasma Physics and Controlled Fusion

PAPER • OPEN ACCESS

JET exhaust detritiation system replacement—design, commissioning, and operation

To cite this article: Robert George *et al* 2023 *Plasma Phys. Control. Fusion* **65** 064002

View the article online for updates and enhancements.

You may also like

- Development of PEFC Low Pt-Loading Graphene Catalyst Layer By Electrospray Method for Increasing Output Power
Masaya Okano, Suguru Uemura and Yutaka Tabe
- An Examination of the Factors That Influence Primary Battery Longevity Performance Under Multiple-Cell Vs Single-Cell Testing Conditions
Jessica Joubert and Ray Iveson
- Impact of Electrode Thick Spot Irregularities on Polymer Electrolyte Membrane Fuel Cell Performance
Min Wang, Grace Rome, Samantha Medina et al.

This content was downloaded from IP address 194.81.223.66 on 19/05/2023 at 09:21

OPEN ACCESS
IOP Publishing
Plasma Physics and Controlled Fusion
Plasma Phys. Control. Fusion **65** (2023) 064002 (19pp)
https://doi.org/10.1088/1361-6587/accecd

JET exhaust detritiation system replacement—design, commissioning, and operation

Robert George[1,*], David Kennedy[1], Tim Huddleston[1], Aarthee Vittal[1], Ryan Morris[2], Simon Ng[3], Xavier Lefebvre[1] and JET Contributors[4]

[1] H3AT Division, UKAEA, Abingdon, United Kingdom
[2] Specialist Consultancy and Laboratory Solutions, Jacobs, Warrington, United Kingdom
[3] Office of the Chief Engineer, UKAEA, Abingdon, United Kingdom

E-mail: robert.george@ukaea.uk

Received 19 January 2023, revised 11 April 2023
Accepted for publication 20 April 2023
Published 2 May 2023

Abstract

The exhaust detritiation system (EDS) of the Joint European Torus (JET) active gas handling system removes tritium from exhaust gases and contaminated air prior to discharge to stack. The system was replaced prior to JET's tritium experimental campaign due to corrosion damage. In this paper, the following topics are presented: system function and description, corrosion and failure of the previous EDS, enhancements for the replacement EDS including testing of acid passivation column, commissioning experience, operating experience and performance. Acids including hydrofluoric were generated in catalytic recombiners following inadvertent halogen ingress. Pitting corrosion was identified with breakthrough failure of condensate pipework. To mitigate a recurrence, a novel acid passivation sub-system was designed. The acid passivation testing demonstrated successful performance of the design and calcium-hydroxide passivation packing tested, with acids below the limit of detectability at the test column outlet. Issues encountered during commissioning are described and key performance metrics such as detritiation factor reported. Finally, operational issues and system performance is presented.

Keywords: catalytic recombiner, molsieve dryer, tritiated water, pitting corrosion, passivation, fusion fuel cycle

(Some figures may appear in colour only in the online journal)

1. Introduction

The most viable route to energy production from nuclear fusion requires use of a deuterium-tritium fuel mix [1]. The Joint European Torus (JET) is the only magnetic confinement fusion reactor currently capable of operating with tritium. Recently a major tritium campaign was performed at JET [2]. Due to the radioactive nature of tritium as well as its scarcity, JET has an active gas handling system (AGHS) to safely store, supply, recover and process tritium.

Part of the AGHS is the exhaust detritiation system (EDS). The purpose of EDS is to remove tritium from exhaust and containment gases before they are discharged to the environment, in accordance with the ALARP (as low as reasonably practicable) principle. The system handles gaseous effluents from both normal and accident conditions and is classified as key safety related equipment for JET [3].

[4] See Mailloux *et al* 2022 (https://doi.org/10.1088/1741-4326/ac47b4) for JET Contributors.
[*] Author to whom any correspondence should be addressed.

Original content from this work may be used under the terms of the Creative Commons Attribution 4.0 licence. Any further distribution of this work must maintain attribution to the author(s) and the title of the work, journal citation and DOI.

© 2023 Crown copyright. Reproduced with the permission of the Controller of Her Majesty's Stationery Office

The design, commissioning and operating experience of the original JET EDS has been previously reported [4, 5] following system installation and use during deuterium–tritium experimental campaign 1 in 1997. Designs and advancements on similar systems—most notably for International Thermonuclear Experimental Reactor (ITER) —are also reported [6, 7]; however the basis of JET EDS remains relevant today as a means of bulk gas detritiation.

In 2017, the original JET EDS suffered mechanical failures due to corrosion. The system was replaced in 2019 and commissioning was completed in 2020, ahead of the tritium boundary expansion (end of September 2020) which marked when tritium started to be injected into the torus. This paper therefore presents several topics:

- System overview of the new EDS (functional requirements and how these are achieved).
- Corrosion and failure of the original plant (inspections and tests conducted: scope, methods, results).
- Enhancements for the replacement plant to mitigate any future corrosion (focused on design and testing of the novel acid passivation sub-system; sizing requirements, performance observed, efficacy achieved).
- Commissioning experience and results (challenges and solutions, performance results including detritiation factor (DF)).
- Operating experience during the recent JET tritium campaigns (system performance, reliability).

This paper highlights the recent changes in design, the viability of new equipment used to mitigate corrosion, and the lessons learnt during commissioning and operation which will be useful to other entities planning to install their own gas detritiation systems.

2. System overview

The EDS uses a two stage process to recover hydrogen isotopes, and therefore tritium, from the waste gas stream, which consists of:

- JET exhaust: air during maintenance,
- JET exhaust: plasma gas/air mix in case of an accident,
- AGHS detritiated impurities (effluent),
- AGHS secondary containment purge gas (nitrogen),
- air from AGHS local exhaust ventilation (LEV) used during AGHS invasive maintenance,
- air from room detritiation in the event of contamination being detected in selected plant rooms.

The first stage of the process is to convert all elemental hydrogen and hydrogen containing species (e.g. methane) to water, by passing the gas through hot, catalytic recombiners. The second stage is to trap the water onto a molecular sieve packed dryer, dehumidifying, and hence detritiating the gas prior to discharging it to the building stack. Once the dryer is saturated, a fresh dryer is put in service. The saturated dryer is put into a closed loop where it is heated to release the water vapour, which is then condensed and drained to a tritiated water storage tank.

2.1. System requirements

The DF, the mass flow of tritium at the inlet versus that at the outlet, is required to be $\geqslant$1000. The system must be available and in-service 24 h a day, 7 d a week. It is key safety related equipment for JET, able to provide suction and detritiation of JET torus exhaust gases in the event of an accident or major plant fault.

The EDS is sized for the same conditions as the original system: to maintain an air in-flow velocity $\geqslant$1 $m{\cdot}s^{-1}$ through a JET main horizontal port used for remote access during torus maintenance [8]. This corresponds to a maximum flowrate of 500 $m^3{\cdot}h^{-1}$ through EDS.

The passivation system requirements are summarised in section 4.

2.2. Equipment overview

The EDS process flow diagram is shown in figure 1.

The system consists of the following parts:

- Inlet manifold, with Premium Analyse C-Ionix tritium monitor.
- Supplementary compressed air feed supplying 42 $m^3{\cdot}h^{-1}$ when measured recombiner oxygen levels are $\leqslant$10%.
- High efficiency particulate filter, size 10 μm Pall HDC II Series candle filters, to filter out any dust/solid matter.
- 2 off 3-phase 60 kW electrical in-line heaters and 2 off counter flow heat exchangers.
- Low temperature recombiner, BASF Puristar R0-20, 0.47% Wt palladium on alumina packed bed (catalyst bed height 200 mm, diameter 700 mm, particle size 2–4 mm), operated at 150 °C, for conversion of Q_2 to Q_2O (where Q corresponds to any of the isotopes of hydrogen).
- High temperature recombiner, BASF Puristar R0-20, 0.47% Wt palladium on alumina packed bed (catalyst bed height 200 mm diameter 850 mm, particle size 2–4 mm), operated at 450 °C, for conversion of CQ_4 to Q_2O (plus CO_2).
- Passivation column (1 duty/1 standby), each packed with high purity calcium hydroxide beads (Intersurgical Loflosorb, passivation bed height 1200 mm, diameter 850 mm, particle size 3–4 mm), for scrubbing out any acids by conversion to salts. Operating temperature 60 °C.
- Condenser for collecting and draining Q_2O when water loading is high, served by 4 °C chilled water.
- Molecular sieve dryer (Siliporite NK 10 4 Å zeolite molsieve packed bed, height 1200, diameter 800 mm, particle size 2.5–5 mm) for capturing Q_2O with high efficiency, operated at ambient temperature.
- Blower: Airtech Vacuum Inc. 3600 max rpm, hermetically sealed, magnetically driven, 15HP three phase motor. EDS flow range min 150 to max 500 $m^3{\cdot}h^{-1}$, nominal flowrate 180 $m^3{\cdot}h^{-1}$.

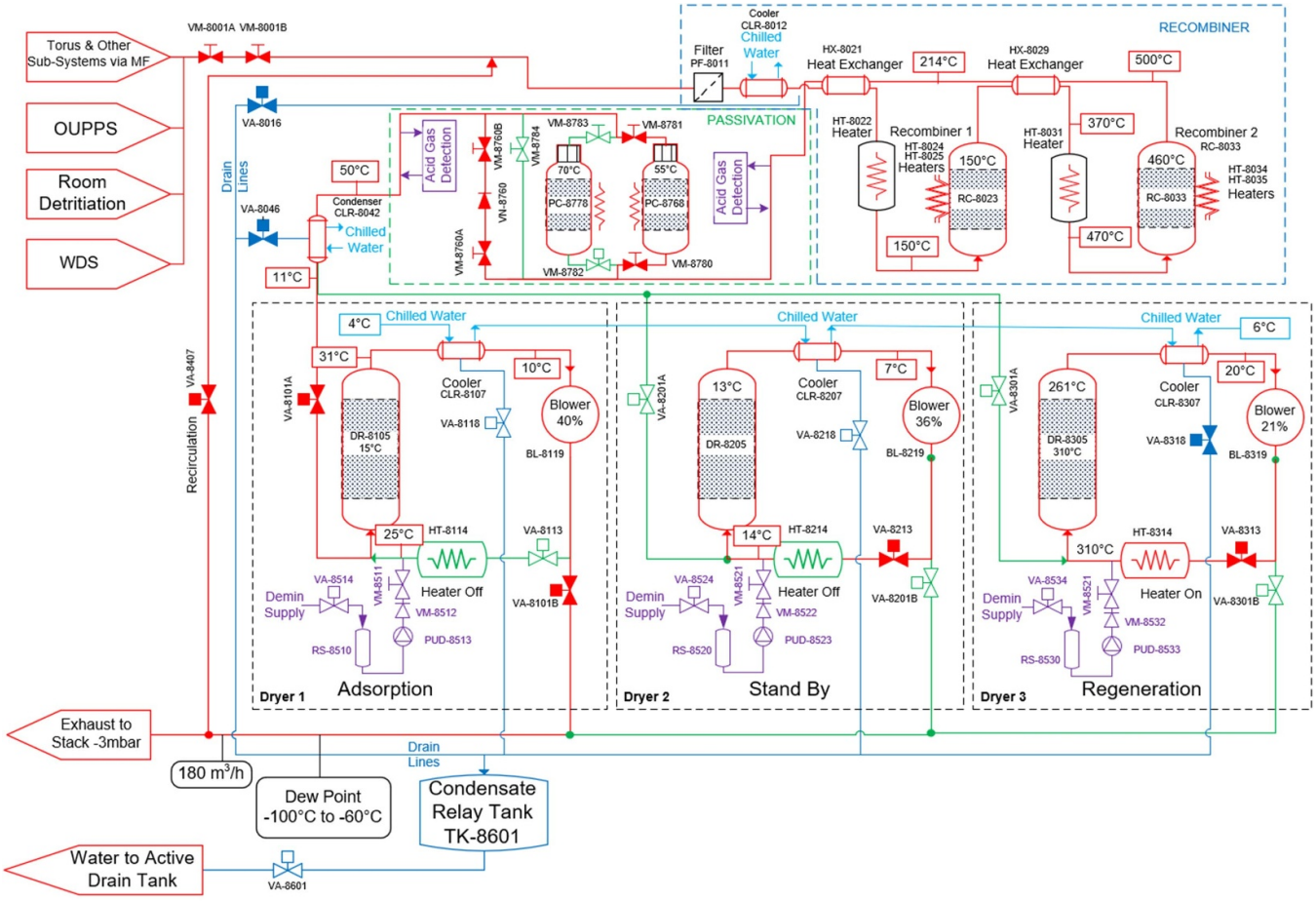

Figure 1. JET exhaust detritiation system process flow diagram, showing typical operating parameters. Dryer 1 in adsorption, Dryer 2 in standby, Dryer 3 in regeneration.

- EDS outlet to stack connection line. Includes GE Sensing Moisture IQ humidity monitor and Premium Analyse C-Ionix tritium monitor.
- Recirculation line allowing portion of EDS outlet gases to return to inlet. Normally gas recirculation mode is on, due to low feed flowrate. When the recirculation line is closed, EDS is in once-through mode which allows higher inlet and outlet flow rate, up to 500 $m^3 \cdot h^{-1}$.
- Condensate relay tank (CRT), collects tritiated condensate from 5 off EDS condensers, capacity 151 l.
- Active drain tank (ADT), HTO holding tank, capacity 4000 l. This is where tritium recovered by EDS is stored, pending treatment by the water detritiation system (WDS) or drumming and dispatch for offsite processing.

The system uses a Siemens SIMATIC S7-400 controller to provide HMI to the operator in the control room, for handling alarms and running sequences.

An independent system of hardwired safety interlocks is additionally in place to cut power/compressed air to the heaters/blowers/actuated valves as required if unsafe conditions are detected. Hardwired interlock testing is performed every 6 months.

2.2.1. Dryer regeneration. When the dryer molecular sieve bed becomes saturated (indicated by rising outlet humidity) a fresh dryer is put into service, whilst the saturated dryer is put into a closed loop regeneration cycle. Each dryer circuit consists of a 60 kW inline three-phase heater, the molsieve bed, a condenser cooled by 4 °C water, and the blower. The heater runs at operating temperature of 310 °C, heat is transferred to the molsieve bed and water is evaporated off the bed, then condensed and drained to the CRT. Once the regeneration is complete (bed outlet temperature reaches its 260 °C setpoint), the heater is shutdown and the circuit cools back to ambient temperature. Pressure and vacuum relief valves are included to manage the changes in circuit pressure during the heating and cooling phases respectively.

3. Corrosion and failure of previous EDS

3.1. Background

In June 2017, the first indication of a significant EDS fault was observed, when a leak of liquid was identified from one of the system's condensate lines into the building. The system was put in shutdown to allow investigation into the source of the

leak. The liquid was analysed and found to contain chlorine and fluorine ions. The EDS system had inadvertently produced hydrochloric and hydrofluoric acids (HCl, HF) which had resulted in damage sufficient to warrant replacement of the system [9].

HCl and HF are highly corrosive and toxic substances. Therefore, hazard reduction and clean-up was first performed, utilising a high degree of risk assessment, work control, personal protective equipment (PPE) and incident response planning in the event of operator injury, in accordance with national health guidance [10]. All liquid inventory was pumped out to temporary storage containers, then the system left vented to allow evaporation of residual moisture.

With only a residual hazard remaining, it was then possible to fully investigate the state of the EDS plant. It was apparent that failure due to corrosion had occurred, so the extent and severity of damage needed to be established, and the exact nature of corrosion and the root cause of this corrosion identified. A summary of the investigation and analysis is presented.

3.2. Visual inspection

3.2.1. Method. Aside from inspection of external damage with the naked eye, internal inspections were performed using a borescope (Olympus Iplex RX industrial endoscope, Model: IV9620RX, Diameter 6.0 mm, Length 2.0 m). A qualified inspector was contracted to perform the inspections with UKAEA staff. Using this equipment, partial views of most components were achieved, often enabled by drilling a hole in pipework to form entry points for the borescope head. To aid gross positioning of the borescope, as well as reduce contamination of the equipment, sections of $^1/_2''$ semi flexible plastic hose were used as guide tubes. The borescope itself has a steerable head to look around, and also includes lighting and zoom capabilities.

3.2.2. Results

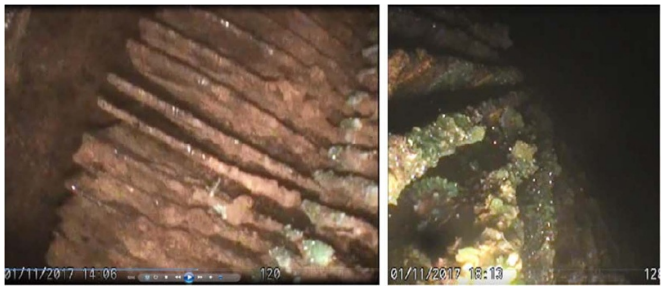

Figure 2. Internal inspection pictures of cooler/condensers' heat exchanger surfaces.

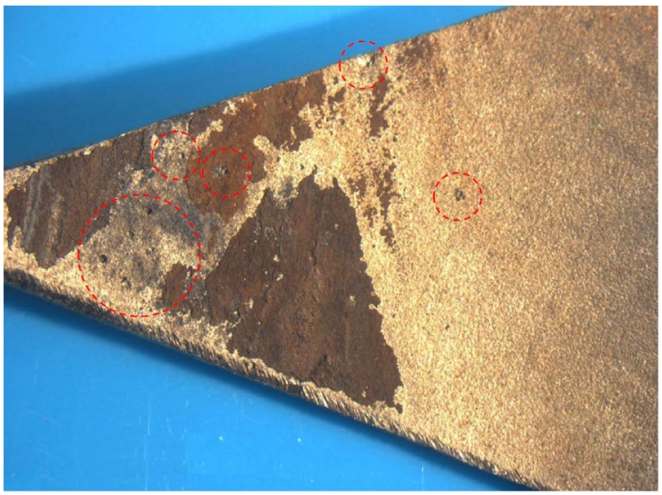

Figure 3. Section of pipework with pitting revealed after partial removal of surface deposits.

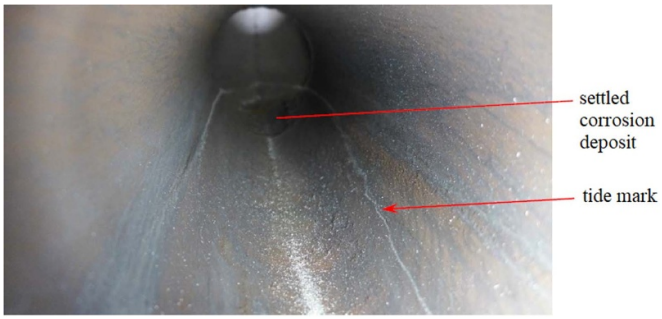

Figure 4. Internal image of 5 inch pipe demonstrating settled deposits and the presence of a tide mark.

3.2.3. Discussion. The visual inspection identified two modes of corrosion—general corrosion and pitting.

Figure 2 is a typical image exhibiting clear indications of corrosion on heat exchanger surfaces. The surfaces themselves were heavily contaminated with debris build-up, corrosion products and crystallised salts. Some surfaces also appeared wet, suggesting deliquescence due to salts present on the internal surfaces.

From figure 3, the colour of the deposit is indicative of iron-based corrosion product (haematite) but the structure of the deposits does not match a corrosion scale growth (e.g. from general corrosion); the 'mud-cracking' feature indicates deposition of fine particles from a liquid. Removal of the deposits revealed substantial pitting and indications of intergranular attack.

Figure 4 shows $5''$ horizontal pipework with tide marks indicating build up of water in the bottom of the line whilst the top of the pipe is in better condition.

3.3. Scanning electron microscopy (SEM)

3.3.1. Method. Selected samples taken from the EDS pipework were taken offsite to Jacob's Active Metallographic Facility and imaged using SEM to help identify corrosion and damage mechanisms. Most samples taken were covered in a pale deposit, in some cases this was removed using industrial methylated spirits, chosen to avoid contamination or alteration of the corrosion features. In other cases, Clarke's solution was used to remove the corrosion product to study the steel substrate condition.

3.3.2. Results

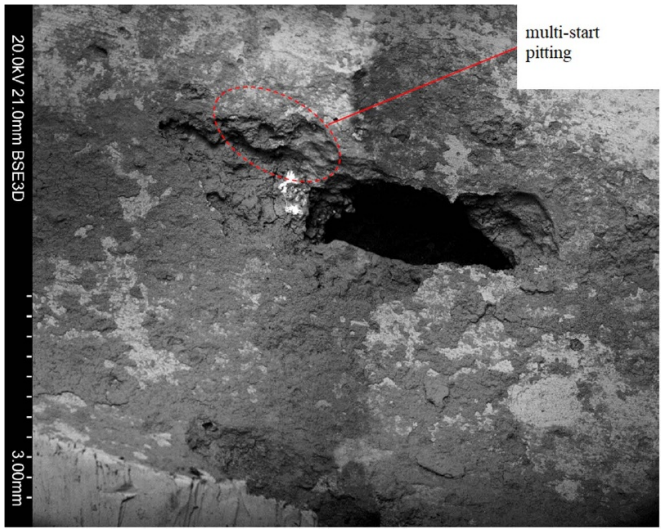

Figure 5. Scanning electron micrograph of perforation (location of pipe failure).

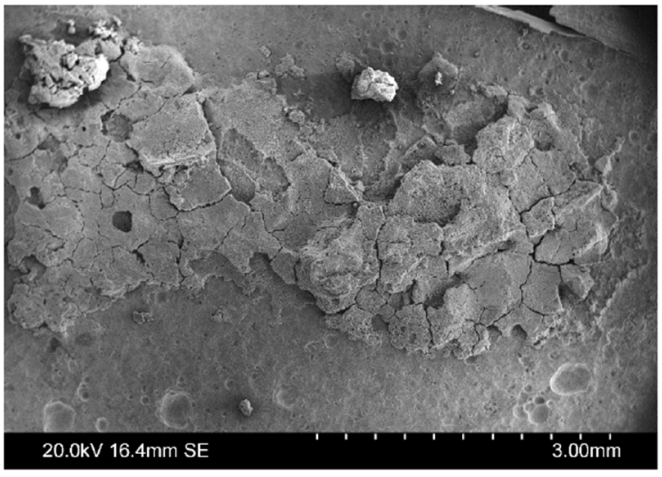

Figure 6. Pitting revealed on sample surface after partial removal of surface deposits using Clarke's solution.

3.3.3. Discussion. Figure 5 is a SEM image of the hole in the $1/2''$ condensate pipe caused by pitting corrosion, this pitting was initiated by deposits of corrosion products, that were not solely generated locally to the hole. These formed occluded corrosion cells where localised anodic corrosion sites experienced stabilised auto-catalytic pitting. Localised thinning in this location was covered by further deposits suggesting an extended operational period following the failure. Figure 6 shows further evidence of pitting corrosion.

As a result of the extensive corrosion observed, the decision made was that EDS repair was not viable. Instead the entire system (up to but excluding the ADT) has been replaced.

3.4. pH and conductivity

3.4.1. Method. pH and conductivity of the ADT water was routinely sampled over several years. These characteristics are typically sampled to monitor for presence of acid and corrosion products within the water. Small samples of ADT water have been extracted and analysed in the onsite laboratory.

3.4.2. Results

3.4.2.1. pH

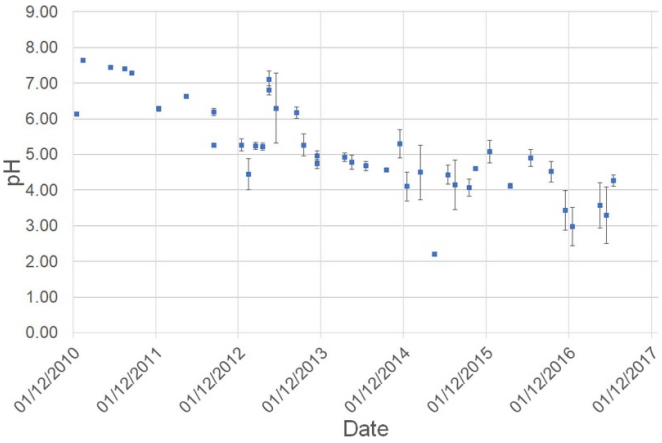

Figure 7. Averaged pH levels from active drain tank samples 2011–2017, including standard deviations.

3.4.2.2. Conductivity

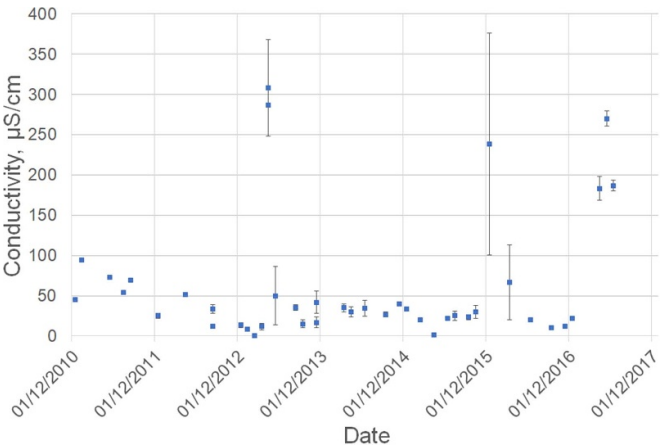

Figure 8. Averaged conductivity from active drain tank samples 2011–2017, including standard errors.

3.4.3. Discussion. Routine liquid sampling (figure 7) has demonstrated a pH as low as 2; upon plotting the data, it can be seen pH has slowly reduced over the years from reading around 6.5 in 2011 to around 3.5 in 2017, at which time EDS failure occurred.

The liquid sample conductivity (figure 8) was relatively stable over time, but with at least one contamination event in 2013, and with an additional anomality in December 2015, likely associated with the installation of the WDS. An order of magnitude increase is observed from April 2017.

3.5. X-ray photoelectron spectroscopy (XPS)

3.5.1. Method. XPS was used to indicate the elemental stoichiometry of various sediments within the system. Sediments dissolved or in suspension in the liquids were analysed by sample evaporation in petri dishes and residual powder analysed using XPS to indicate quantity and chemical state.

Sediments representative of solid materials from several locations were also gathered and analysed by XPS.

3.5.2. Results

3.5.2.1. Evaporated wet samples

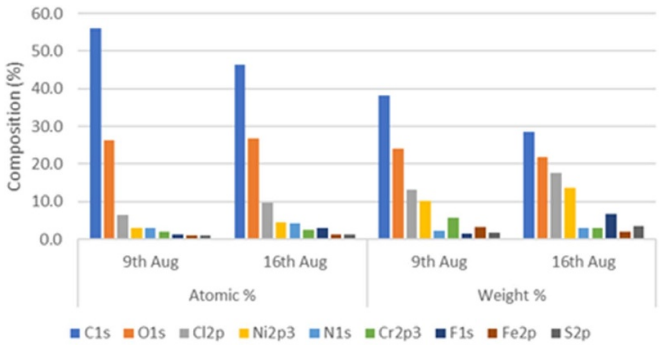

Figure 9. Chemical analysis of evaporated active drain tank samples.

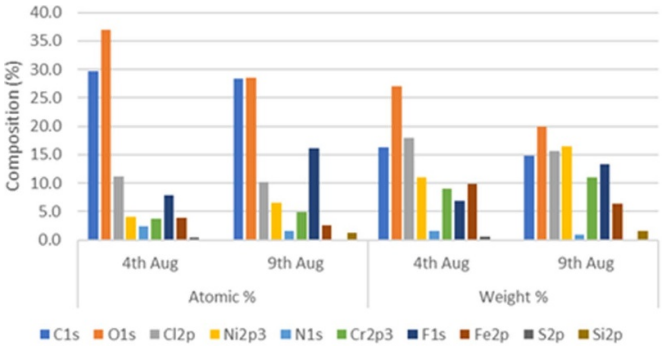

Figure 10. Chemical analysis of evaporated condensate relay tank samples.

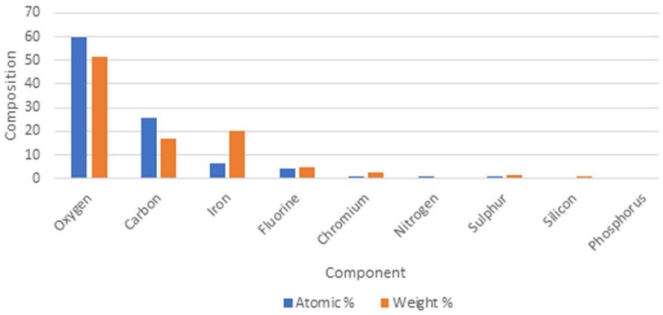

Figure 11. Surface composition by x-ray photoelectron spectroscopy of active drain tank slurry.

3.5.2.2. Solid material sampling

Table 1. X-ray photoelectron spectroscopy analysis of Pigmat with faulty valve residues.

Name	Peak BE	Atomic %	Weight %
Oxygen	532.3	44.3	38.3
Carbon	285	33.4	21.7
Silicon	102.6	10.2	15.5
Fluorine	684.8	4.5	4.6
Iron	711.6	3.8	11.4
Chromium	577.8	2.3	6.5
Nitrogen	400.1	0.5	0.4
Sulphur	169.2	0.5	0.8
Chlorine	198.7	0.4	0.7

Table 2. 20 cm 1/2″ pipe analysis by x-ray photoelectron spectroscopy.

Name	Peak BE	Atomic %	Weight %
Oxygen	531.26	45.9	35
Carbon	284.97	28.8	16.5
Fluorine	684.44	9.3	8.4
Iron	710.97	7.9	20.9
Chromium	577.36	5.1	12.7
Silicon	102.15	1.6	2.2
Nickel	853.46	1	2.8
Molybdenum	232.47	0.3	1.2
Chlorine	198.28	0.2	0.4

Table 3. X-ray photoelectron spectroscopy analysis of green deposits from condenser.

Name	Peak BE	Atomic %	Weight %
Fluorine	685.19	39	30.4
Carbon	284.89	21.1	10.4
Oxygen	532.97	18.2	11.9
Iron	712.23	10	22.8
Nickel	858.07	7.3	17.4
Chromium	579.22	2.2	4.7
Silicon	96.8	1.1	1.3
Nitrogen	400.21	0.7	0.4
Chlorine	199.35	0.5	0.7

3.5.3. Discussion. The XPS results are discussed below. The molecules or compounds are not determined from the measurement technique alone, as such these have been hypothesised based on reasonable assumptions and the known physicochemical properties.

3.5.3.1. Wet samples. The XPS results identify the elements present within the wet samples taken from EDS. For the ADT (figure 9) and CRT (figure 10) there are fluorides and chlorides, all bound to cations, nitrogen bound up as mixed quaternary ammonium salts, nitrates and amines. All metallic components were found to be in ionic, non-metallic states, bound to a mixture of chlorides, fluorides and oxides.

The chrome is likely to be Cr(III) chloride, based on its binding energy, with the stoichiometry noted, the abundance of oxygen and the deposit colour, and water seen. This is likely in its dark green hexahydrate form, $CrCl_3(H_2O)x$.

The nickel is likely to be bound to both fluorine and chlorine, the binding energy shift between these two states for this element is small. Stoichiometry suggests there is a saturation of the NiF_2 compound, which is a stable ionic fluoride compounds in air. Nickel halides are green, as is the hydrate $NiF_2.6H_2O$, on drying this can form the yellow dihydrate.

From the binding energy of the Fe seen this is likely to be Fe(III) oxide, this is brown in colour.

Samples of slurry (figure 11) taken from the bottom of the ADT tanks were analysed and were found to be, ignoring the carbon over layer, predominantly Fe(III) oxide, with small amounts of likely Cr(III) fluoride.

3.5.3.2. Solid samples. Table 1 is for deposit from a failed CRT sample isolation valve: carbon and organic silicones plus organic nitrogen are associated with Pigmat material. Fluorine is evident in an ionic state. Cr and Fe are present, both in a non-metallic state. From the binding energies and stoichiometry seen the chromium is likely associated with the halides, where Cr(III) fluoride trihydrate is a green colour and Cr(III) hexahydrate is violet. The iron predominantly is likely Fe(III) oxide.

Table 2 presents XPS of a section 20 cm pipe, demonstrated adventitious and other carbon chemistry, some associated with silicones but displaying a lot of the chemistry of corrosion products associated most likely with the sediments; with large amounts of oxides and fluorides present and a small amount of chloride, along with associated metallic cations used in stainless steel.

Table 3 shows a large presence of fluorine, this is bound to iron, nickel and chromium, which is found in their hydrate states and accounts for the colour. The results suggest corrosion was caused by stainless steel interaction with HF.

3.6. Elemental/ionic analysis

3.6.1. Method. The 'elemental/ionic analysis' was performed by ESG, now SOCOTEC UK Ltd, using the following techniques:

- Inductively coupled plasma (ICP) atomic emission spectrometers.
- ICP mass spectrometers.
- Ion chromatography.
- KONENS—Direct analysis using discrete colorimetric analysis.

3.6.2. Result

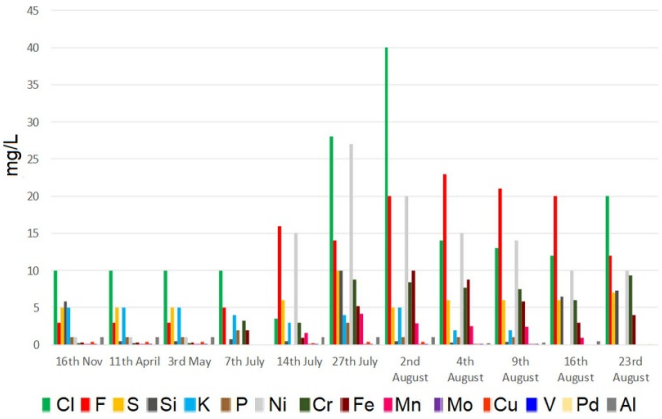

Figure 12. Ion concentration in the active drain tank.

3.6.3. Discussion. Elemental and ionic analysis of ADT water is shown in figure 12. The Cl levels after passing through the AGHS are at 10 mg l^{-1} from the 16 November to 7 July. There is also 2 mg l^{-1} of fluorine until the 7 of July where it doubles to 5 mg l^{-1}, corresponding to an increase in Cr and Fe. The 14 July sample shows a decrease in Cl but a rise in F and Ni also increases. From 27 July sample other components associated with 316 stainless steel construction (Fe, Cr, Mn) also rise correspondingly. The data shows the evolution of halogen ingress and corrosion with time, with increased amount of corrosion product reaching the ADT by 27 July.

3.7. Cause of corrosion and failure

In EDS, complex chemical compounds are broken down, in the high temperature recombiner at up to 500 °C. As the process stream cools by passing through heat exchangers corrosion became evident. In the downstream condenser, a large amount of corrosion had occurred. The corrosion was caused by the presence of aggressive anions, such as fluorine, chlorine and sulphur, causing general and pitting corrosion. Some of these ions remain in aqueous form and continue along the process to the CRT and the ADT, where they are seen in the historical data. There was an abundance of nickel seen in relation to other constituents of stainless steel, this could be due to many historical events occurring and causing the steel to form passivating nickel layers on the surfaces [11]. In air this produces loose films [11]. The water solubility of nickel halides is relatively high, in comparison to other halide salts, in the region of 40 mg l^{-1} (NiF_2) at 25 °C [12]. Additionally, there could be a sensitisation effect being caused due to the release of hydrogen in the reaction of Ni + HF/HCl leading to increased potential for pitting corrosion to occur [13–15].

There could also be a possibility that the beta decay of tritium is changing the electrochemical environment and changing the corrosion properties of the steel [16].

Thin walled drain pipework is particularly sensitive and was where the leaks occurred. Once the first perforation occurred air was drawn into the system causing a hydraulic lock and allowed the large condenser to fill, this process collected historical deposits which contributed to the increase in chemical content seen in the ADT sampling. This process likely also caused the CRT valve to fail, possibly contributing to the escape of liquid past the valve and the build-up of sediment. This also allowed a flow of water to collect in the 5″ pipes which was evidenced by tide marks and sediments. It is likely that the initial failure was caused by the presence of chloride ions, noted in the historical ADT data at a higher concentration than fluoride, as multiple pitting levels were seen throughout the system with much of it re-passivating. HF at low levels will react with nickel, found in the stainless steel to form a passivating NiF_2 layer, these can offer limited protection, preventing further corrosion by halogens.

3.8. Corrosion and failure: conclusion

The EDS system will crack unwanted substances to their ionic forms leading to corrosion downstream. Thin-walled pipes were most susceptible to failure.

Evidence of chlorine and fluorine ingress has been reported, chronically over several years and in discreet events, observed in ADT pH data.

Only aqueous corrosion is noted. Aggressive anions in sufficient concentration caused autocatalytic pitting corrosion in thin-walled pipes leading to perforation. Chloride and sulphur ions were seen in the region of the pitting perforation. An abundance of nickel was seen in relation to other stainless-steel components. HF (and HCl) at low levels will react with nickel, found in the stainless steel to form passivating NiF_2 and $NiCl_2$ layers.

4. Anti-corrosion enhancements for replacement EDS

4.1. Introduction

The replacement EDS was designed with new equipment to detect and mitigate the impact of acid ingress / production. This section presents information on the main equipment installed to perform these duties: section 4.2 describes the passivation system, for scrubbing of acids from the gas stream. The requirements, design, bench validation testing and results are presented. Section 4.3 describes the acid gas detection system, for detection of acids, upstream and downstream of the Passivation System. The requirements, optioneering, design and installation are summarised.

A few other enhancements were also made which are briefly described here. A conductivity monitor (supplied by Automated Waste & Effluent Ltd, D2 Conductivity Cell with C3630 transmitter, range 0–2000 μS) was installed on a stainless steel dip probe on the CRT. The purpose is to detect rises in water conductivity within the tank which may indicate the presence of corrosion product within the condensate. The reading has been stable throughout the EDS operation.

Since the condensate line from the condenser cooler downstream of the recombiners was the source of the breakthrough corrosion, the equivalent line on the new EDS was fabricated out of Hastelloy C-2000 as an additional layer of protection, which is much more resistant to acid than stainless steel that the EDS is mainly composed of.

Purposely built stainless steel corrosion coupons were fabricated and installed in several places within the EDS gas circuit. Each is sited on a removable flange, each site doubling as an inspection port. These flanges can only be broken however, and corrosion coupons removed for analysis, when EDS is out of service. Therefore in practice, these will not be analysed unless EDS has been taken out of service for a significant operational or safety concern.

Equipment specifications also included design requirements to minimise pooling and help prevent build-up of deposit, e.g. by having an increased slope on drain lines and ensuring internals had smooth surfaces and curved edges where possible.

4.2. Passivation system

The passivation system is sited downstream of the recombiner heat exchangers, before the condenser (see figure 1). Since this was an untested technology being installed in a safety critical system, performance validation testing was required, the methodology and results of which are described. The aim was to prove acid removal under foreseen loading conditions and demonstrate stability of the passivation media, which was achieved using a scaled test rig with several passivation media tested.

4.2.1. Passivation requirements. The main requirement of the passivation system is neutralisation of acid, specifically HF, HCl, H_2SO_4 and HNO_3. Two scenarios were considered to determine sizing requirements: acute and chronic acid ingress. A single passivation bed has to withstand five acute events (one hour each, 1 $kg{\cdot}h^{-1}$ of acid), or a 10 month chronic loading (1 $kg{\cdot}month^{-1}$).

The other requirement on the passivation system is to not compromise the flow through EDS. This is one of the key requirements that must always be met for EDS to be available. This corresponds to stability of the passivation media under all foreseen operating and acid loading conditions.

4.2.2. Design. Tyne Engineering performed the sizing of the passivation bed. Sizing of the packed bed assumed a solid–gas interaction limited by external mass transfer control and chemical reaction control. The most demanding conditions in this case were chosen: (acute ingress, HCl (slowest reaction rate with $Ca(OH)_2$), 150 $m^3{\cdot}h^{-1}$ flowrate chosen because this corresponds to highest acid concentration in gas stream).

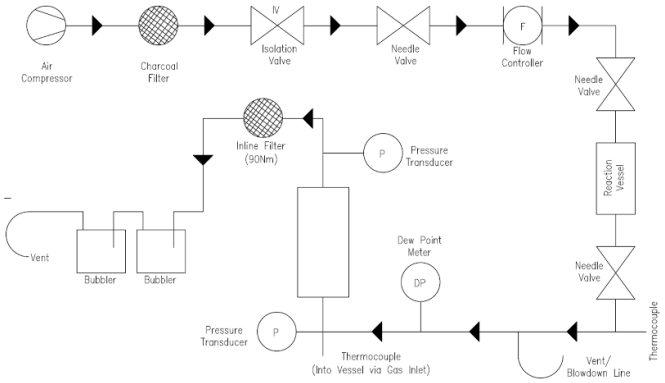

Figure 13. Process flow diagram for passivation scrubbing system experimental verification rig.

The chemical reaction rate constant (per unit surface area of the solid) $k_s > 1 \times 10^{-3}$ m·s^{-1} was taken from [17], where $m =$ mass of solid reactant (g).

The mass of passivation media, and bed length was determined: 555 kg of media, depth 1.2 m (on top of 0.1 m layer inert beads), diameter 0.85 m. The conversion over the 10 year life of the bed was calculated as 3.5%–4.0%.

In order to meet the second requirement the following design elements were incorporated:

- Outlet HEPA filter (10 μm Pall HDC II Series), to prevent any dust or debris carry over.
- Differential pressure monitoring on both the bed and outlet filter, to identify any pressure drop increase with time.
- Jacket heater to prevent condensation forming within the bed.
- A redundant bed (with all above mentioned equipment) available in the event of premature aging or blockage in bed 1.
- A manually selectable bypass route in the event neither bed is available.
- An auto bypass with sprung non return valve set at 30 mbar—to provide continuous EDS flow in the event of the duty bed becoming blocked suddenly.

4.2.3. Performance validation testing. Since the use of soda lime in this type of plant was novel, a scaled rig was built in order to prove that the requirements above—acid removal and bed integrity—could be met. Jacobs was contracted to design, build and operate the test rig.

4.2.3.1. Design of test rig. A PFD of the rig is shown in figure 13.

The rig had two identical assemblies, including:

- Air compressor, for air supply.
- Mass flow controller, controlling flowrate to 10.4 l·min^{-1}, corresponding to plant relevant linear bed velocity of 264 m.h^{-1}.
- Reaction vessel, with acid mixture.
- Pre-heater, for gas feed temperature of 67 °C.

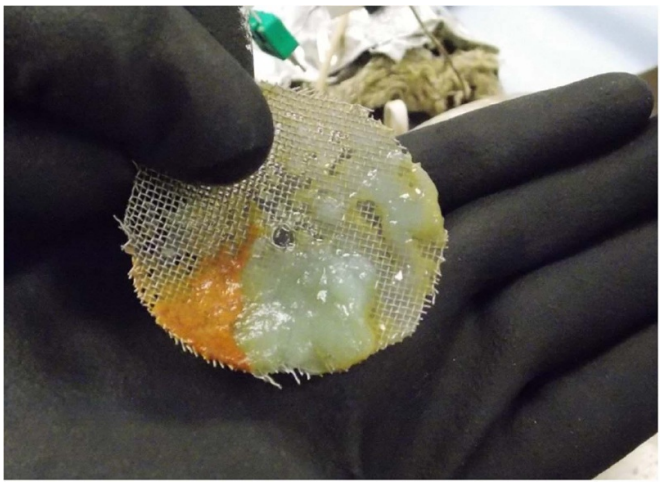

Figure 14. Gel deposit on test column diagrid produced during acute HF testing Intersorb.

- Test column, containing 0.1 m inert material at the bottom for flow distribution with 1.2 m of soda lime for acid neutralisation.
- Two bubblers in series to trap any ionic species breakthrough from the column top. Each had 1 M sodium hydroxide to neutralise acid. This was checked using ion chromatography to determine anion concentration.

Perfluoroalkoxy polymer was used for tubing and 316 Stainless Steel for fittings and the test column. Hastelloy C276 was used for the reaction vessels.

4.2.3.2. Testing and results phase I. The original scope was testing the proposed soda lime media (Intersurgical Intersorb) against several types of acid, under both chronic and acute loading conditions.

Tests performed with HCl and nitric acid were successful. Detection of acid ions within the bubblers was minimal.

During HF testing, flow blockage was encountered. Upon inspection of the column, a gel like substance (figure 14) had been produced which was causing the soda lime balls to clump together and reduce flow path. Heavy build-up of deposit was observed on the inlet tube (figure 15). The soda lime was deemed incompatible with HF, the probable cause being the sodium hydroxide content present within the soda lime, as suggested by the high sodium content of the gel.

Corrosion of the test rig was observed, severe at the bottom (figure 16) and light pitting at the top (figure 17, the latter thought to be caused during rig commissioning).

4.2.3.3. Testing and results phase II. The next phase focused on testing three alternative candidate medias that were available on the market, Nordkalk Verdal, Nordkalk KPAB and Intersurgical Loflosorb, against HF and HCl for a range of chronic and acute cases. These were all calcium hydroxide products with differing levels of impurities.

Acute testing of Verdal and KPAB displayed similar behaviour to the Intersorb. Pressure drop increased during the tests

Figure 15. Corrosion product build-up on bottom flange and inlet pipework during acute HF testing Intersorb (note larger penetration was not used).

Figure 16. Corrosion within the inlet of the test rig column during acute HF testing Intersorb.

Figure 17. Light pitting corrosion on outlet flange during acute HF testing Intersorb.

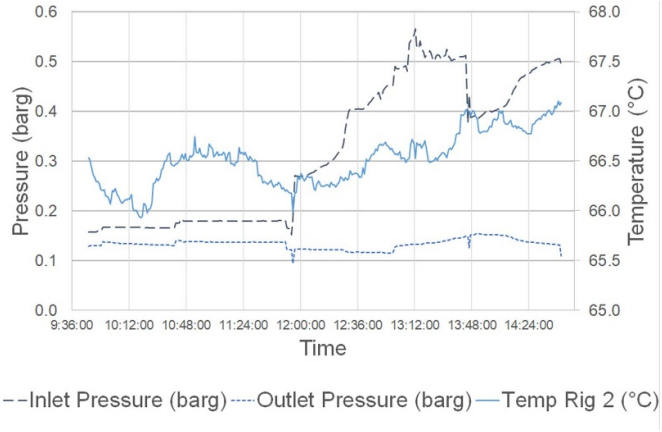

Figure 18. Inlet pressure rise observed during acute HF testing of KPAB on 26 November 2018.

(figure 18) and gel/deposit was observed at the base of the column in each case. Verdal performed slightly better.

A chronic test of Verdal was conducted, for four weeks; no acid was detected at the column outlet during this time. However, inspection of the rig identified a green residue around the bottom (figure 19).

Acute and chronic testing was performed on Loflosorb, which is free from potassium- and sodium hydroxide. Performance during these tests was good, both in terms of no detectable acid at outlet, and stable pressures throughout the tests (figure 20). A very fine layer of light deposit was observed on the inlet flange (figure 21), note that the raised areas of deposit towards the right hand side are bubbles, not thick deposit.

4.2.3.4. Testing and results phase III. The final phase was an 'accelerated chronic' test, to demonstrate equivalent loading from a full 10 month chronic event, but condensed over two or three weeks testing. As well as scaling acid loading, water vapour and CO_2 were injected with dosing equivalent to 10 months within the 2 or 3 week test. Flowrate through the column was 35 $l{\cdot}min^{-1}$. This stressed the test rig, with significant corrosion occurring in the inlet pipework, causing blockages that required periodic clearing to allow testing to continue. The impact on pressures can be seen in figure 22.

Whilst corrosion deposit was observed at the column inlet, the Loflosorb itself was in good condition (figure 23). No

Figure 19. Green residue build-up on bottom flange following chronic HCl testing of Verdal.

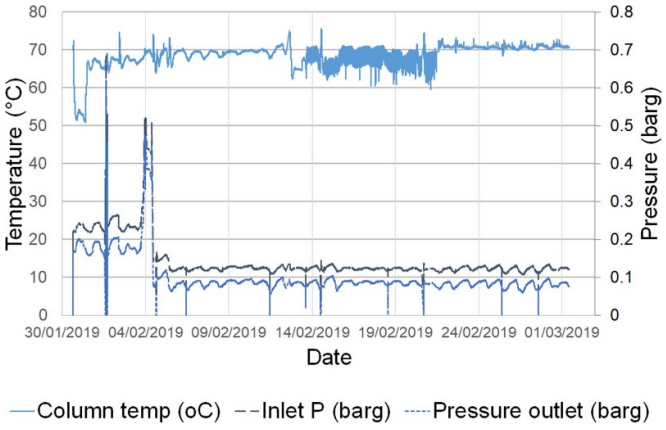

Figure 20. Chronic HF/HCl mix test with loflosorb. Pressures remained stable throughout testing.

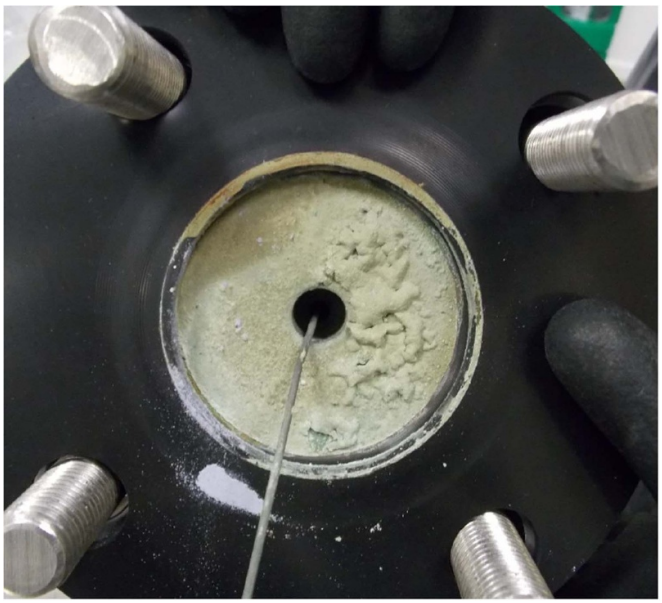

Figure 21. Thin layer of deposit on bottom flange following chronic HF/HCl mix test with Loflosorb.

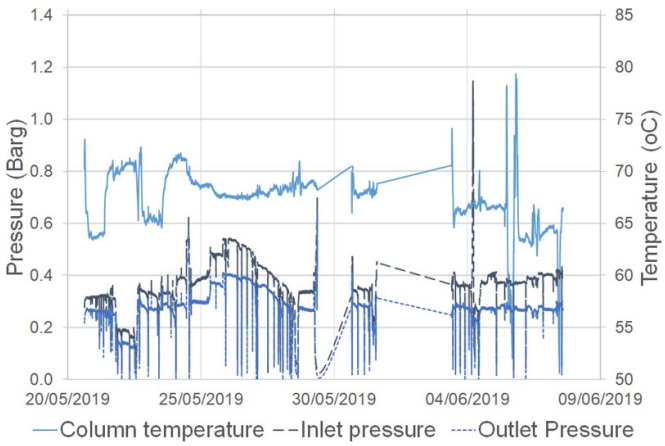

Figure 22. Accelerated chronic test trend for Loflosorb.

corrosion was observed at the column outlet (figure 24) and no breakthrough acid detected in the bubblers. The result of two week and three week tests were consistent. The three week test ultimately had equivalent of 14.6 months chronic acid loading.

Following this final test, the Loflosorb was formally approved for use by UKAEA.

4.3. Acid gas detection system

In addition to the passivation system, there is also an acid gas detection system that needs to monitor for presence and concentration of acids in gas form, upstream of the passivation system, and downstream, to confirm the neutralisation of acid where present. Detection of HF and HCl is required, as well as H_2SO_4 and HNO_3 acid if feasible.

4.3.1. Optioneering. Two main means of acid detection were considered: spectroscopy and chemical-based.

The spectroscopy options were investigated, but ultimately rejected due to uncertainty in the ability of the techniques to detect tritiated acid compounds such as TCl and TF. Spectra for such gases are not known empirically. The equipment also was relatively expensive and may have had tritium compatibility issues.

Use of electrochemical cells was considered a more suitable option. Such equipment would detect all hydrogen isotopic variations of the target acids since all have nominally identical chemical reaction behaviour. The equipment is also relatively simple, robust and affordable.

4.3.2. Design. Honeywell Satellite XT electrochemical cell technology was chosen for the design. For both upstream and downstream of the passivation system, the design consisted of two (duty/standby) manifolds with cells for HF, HCl and SO_2 detection. An H_2SO_4 detecting cell was not available, so SO_2 was selected on the basis that production of SO_2 would occur in recombiners additional to any H_2SO_4, which is a more

Figure 23. Following accelerated chronic testing, Loflosorb (purple balls) came out in good condition.

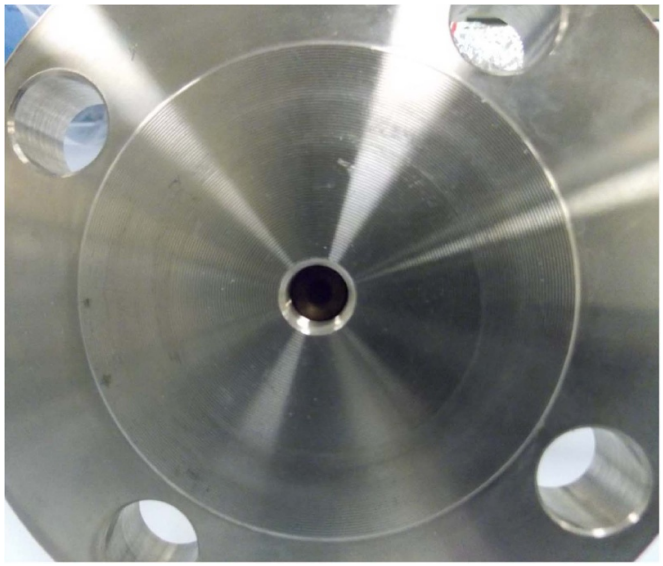

Figure 24. Following accelerated chronic testing of Loflosorb, outlet flange was clean and free from corrosion.

complex molecule. No nitric acid cell was available and this was agreed not required based on the cause of corrosion in the original EDS system not being linked to nitric acid.

The equipment was specified for detecting in the range 0–50 ppm upstream of the passivation system and 0–10 ppm downstream. The limit of detection is 0.5 ppm.

The cells require the following conditions for correct operation: temperature −20 °C–40 °C, pressure 0.7–1.3 bar(a), humidity 15%–90% RH, gas velocity approx. 0.5–3.0 $m \cdot s^{-1}$.

4.3.3. Installation. The acid gas detection assemblies were manufactured and installed by 2019. The combined cost of materials and fabrication was higher than anticipated, making the spectroscopy based solutions more competitive (based on price) than originally determined. The material and fabrication costs could have been reduced by utilising a much smaller line size, as often used for sample-loop instrumentation systems, with addition of a pump to achieve the necessary velocities past the sensors; instead of the passive design opted for which utilised 1″ diameter lines.

A concern identified after the design completion was the risk of electrochemical cells being pulled by vacuum out of their housing into the gas stream. To prevent this, epoxy resin is used to fix the cells into their holders. This effective, but non-optimal solution has meant that the holder requires replacing as well during routine cell replacement, which also raises the ongoing system operational expenditure.

Operational performance is presented in section 6.

5. Commissioning of replacement EDS

Design and fabrication of EDS started in 2018, with FAT and delivery of the 5 skids to Culham in 2019. The majority of equipment was delivered through contract with Tyne Engineering of Canada, with onsite installation works performed primarily by Jacobs Field Services. Commissioning commenced later in 2019, with non-active operational and performance testing. Active commissioning was then performed in the summer of 2020, after which EDS was put into service.

This section highlights some of the challenges encountered plus results of key tests performed to prove EDS met its functional requirements.

5.1. Challenges

5.1.1. Blower bearings. Blower bearings failed early on during the commissioning phase, the possible cause following supplier investigation was over-use of grease during assembly, plus inconsistent torquing of fixtures and fasteners. For all three units, the supplier replaced the bearings (with custom-made hybrid ceramic/nitrogen infused bearings), changed the type of grease (to Lubcon Ultratherm LS 1502) and also specified a different shipping orientation. Following reinstallation, vibrations were once again seen for one of the three blowers. Investigations continued and further inspection and remedial work was performed by UKAEA. All three blowers have performed well since, with vibration monitoring equipment now installed to detect any changes with time. Blower 2 has displayed more noise than the other two, however no cause has been identified and the trend has not become significantly worse over the past 2 years. Further more specific vibration monitoring indicates that the vibration is at the drive end motor bearing.

5.1.2. Condensate drain blockage. During initial proving of the condensate lines from one of the condensers to the CRT, water failed to drain properly. Investigation identified swarf or other small debris within the condensers had caused the blockage, compounded by a reduction in pipe internal diameter at the CRT interface (due to pressure vessel code compliance). The blockage was removed, equipment cleaned and

Figure 25. Condenser outlet camera showing the dam installed for Dryer 3. Water droplets and a pool forming can be seen during regeneration on 8 June 2020.

new strainers fitted on each drain line in order to prevent a recurrence.

5.1.3. Water carry-over. During regeneration cycle tests, water carry over past the condenser to the blower was observed. This was evidenced by the thermal mass flowmeter returning an overrange error due to moisture ingress increasing the heat capacity of the fluid, and increased vibration of blowers. Indeed, water was found in the base of one blower casing during invasive investigation. A camera was installed at the outlet of the condenser and water could then be seen as droplets 'raining' through the pipework during the dryer regeneration (figure 25). The solution consisted of the installation of a dam on the outlet of each condenser, to reduce the carry-over, and lowering the blower speed during the regeneration cycle.

Tests were conducted watching the camera in real-time, to determine the maximum possible flowrate without water droplets visibly going over or hitting the dam. This solution was effective, but the dryer regeneration is approximately twice as long (from 15 to ∼30 h) due to the reduced blower speed.

5.1.4. Vacuum relief valve failure. During a dryer regeneration cooldown, the vacuum relief valves failed to operate at the opening pressures, so the pressure dropped to 380 mbar(a), sufficient to syphon water back up from the CRT. The water flooded the condenser and ran down to the blower, eventually tripping the blower on high inlet temperature. Figure 26 shows the pressure drop (PI-8303) and CRT water level (LI-8601) as a function of time.

The valves were removed for inspection and confirmed to require higher differential pressure than specified to open. Half of the valves have been replaced with valves with metal to metal seats, and all were recalibrated with lower opening differential pressures. Software modifications were also made to

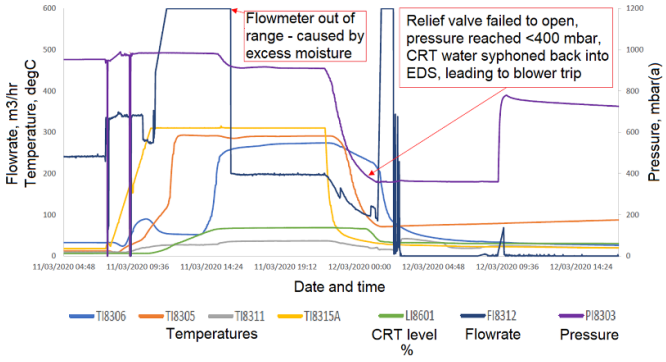

Figure 26. Dryer 3 regeneration: ingress of water from condensate relay tank, 12 March 2020.

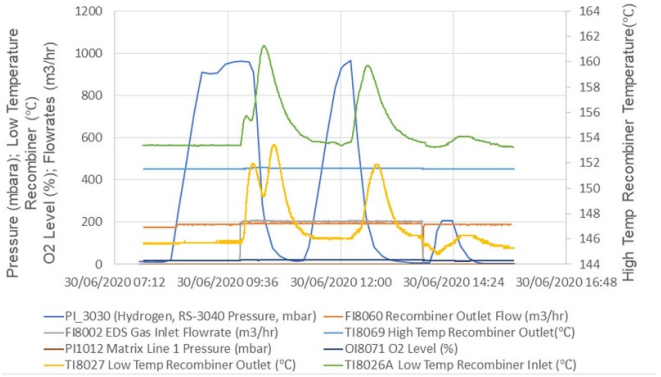

Figure 27. Flammable gas test with hydrogen.

close the condenser drain valve during regen cooldown or if pressure <600 mbar(a) is detected in the dryer circuit. No similar incidents have occurred.

5.2. Inactive commissioning tests

During commissioning, various tests were conducted to prove the functionality and performance of the EDS. Results of key tests are presented here.

5.2.1. Recombiners. In order to confirm and characterise catalytic performance, the recombiners were tested with hydrogen and methane to observe the temperature transients caused by the exothermic reactions with oxygen. The gas fed to EDS was 95 vol% nitrogen, 5 vol% H_2 or CH_4. Figure 27 shows the behaviour for hydrogen, with low temperature recombiner rises of 6 °C – 8 °C for 2 off injections of ∼100 bar·L H_2 at a total gas flowrate of 200 $m^3 \cdot h^{-1}$. Figure 28 shows the behaviour for CH_4, with high temperature recombiner rises of 12 °C – 16 °C for 2 off injections of ∼100 bar·L CH_4 at a total gas flowrate of 200 $m^3 \cdot h^{-1}$.

5.2.2. Dryers. Dryers were tested with atmospheric air to determine their ability to remove moisture (observing the outlet dew point) as well as water holding capacity. This data provided a baseline for dryer performance which informs the operating regime. In this mode of operation, dryers ran for 48 h

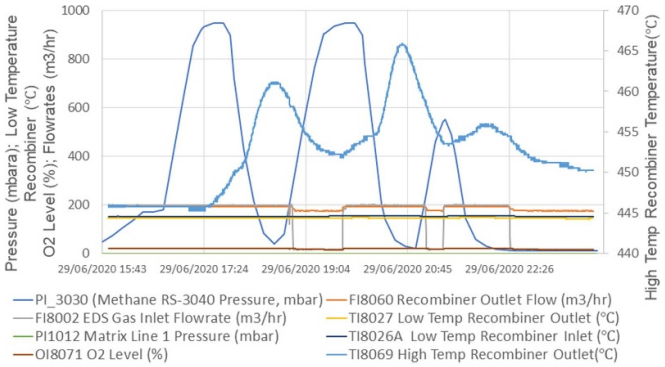

Figure 28. Flammable gas test with methane.

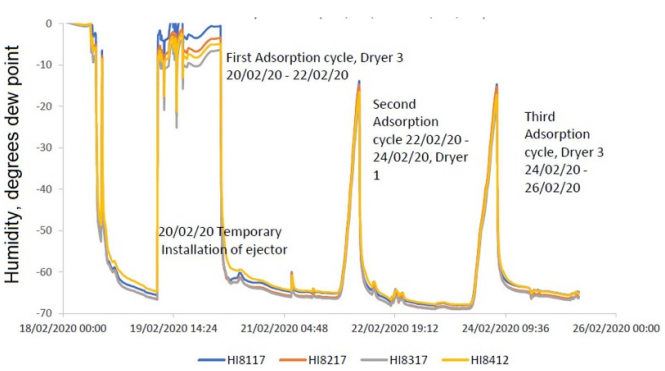

Figure 29. Humidity trends during commissioning.

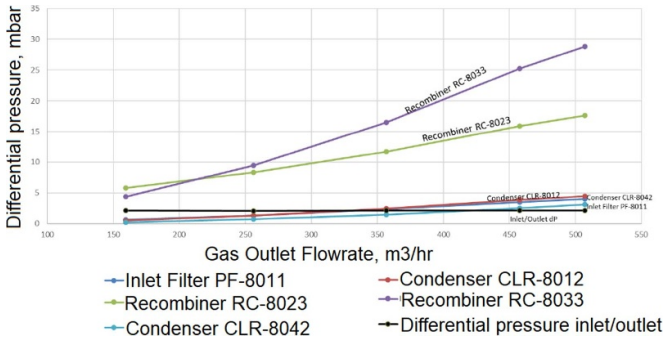

Figure 30. Flowrate vs differential pressure, operation in once-through mode.

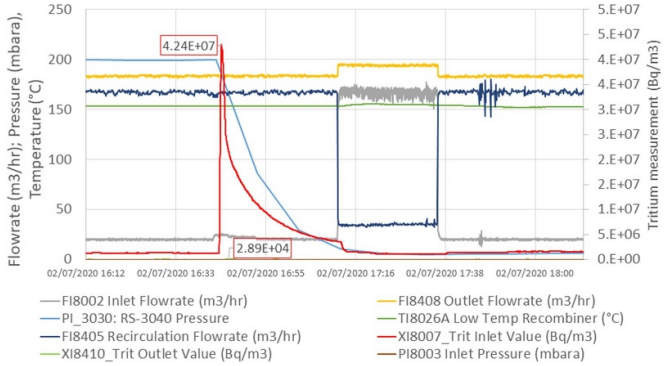

Figure 31. Active commissioning tritium test.

before rising humidity on the outlet indicated bed saturation and a fresh dryer put into service. Outlet humidity was between −60 °C and −70 °C dew point (figure 29), which corresponds to ∼5 ppm(v) water in air. The largest amount of water captured in a molsieve bed was 120 l.

5.2.3. Pressure drops. The pressure drops across certain pieces of equipment were monitored across the range of blower operating speeds. Pressure drop increases with increased flowrate through the system. It can be seen from figure 30 that the largest pressure drops occur across the recombiner beds. The measured pressure drops were all within an acceptable range, and a baseline was established which could be used to identify changes of equipment condition which cause the pressure drop increasing to outside of the range, e.g. a partial blockage.

5.2.4. Passivation packing inspection. At the end of the non-active commissioning phase, the passivation bed filters were replaced. The condition of the used filters was very good, with no sign of dust or debris build-up from the passivation beds. A visual check of the top of the passivation bed was also performed and the calcium hydroxide pellets were confirmed to be in good condition with no signs of degradation.

5.3. Active commissioning

5.3.1. Detritiation tests. A small quantity of tritium was introduced to the EDS to observe the detritiation performance.

The gas mix was pumped from AGHS with EDS inlet flowrate of 21 $m^3 \cdot h^{-1}$. Towards the end of the test, EDS was put in once-through mode (167 $m^3 \cdot h^{-1}$) to observe any difference in detritiation. The test is presented in figure 31. Inlet tritium concentration peaked at 42.9 $MBq \cdot m^{-3}$. There was no observable change in outlet tritium concentration compared to the background average reading of 15 $kBq \cdot m^{-3}$, indicating successful capture of the fed tritium.

To observe the DF, three water bubblers were installed for the test duration. The sampling locations were (1) upstream of the recombiners on inlet line, (2) downstream the recombiners, between condenser and the duty dryer and (3) downstream of the duty dryer on the outlet line to the building stack (table 4).

The EDS DF was calculated as the sum of total tritium activity at sampling location 1, divided by the total tritium activity at sampling location 3: 10 700. This is an order of magnitude above the required DF of 1000. It must also be noted that the activity detected at sampling point 3 during the test is identical to the background reading taken prior to the test, meaning the outlet activity may be even lower, and DF even higher.

The DF across the recombiners is the sum of total tritium activity (excluding HTO) at sampling location 1 divided by

Table 4. Commissioning bubbler data.

Sample reference	Sampling location	Tritium species	Specific tritium activity (Bq/l H_2O)	Total tritium Activity (Bq)
J-21124.1	EDS inlet	HTO	231 600 ± 6950	5450 ± 370
J-21124.3		HT	28 570 ± 858	615 ± 41
J-21124.5		HT (overflow)	5611 ± 169	119 ± 7.9
J-21124.7		CH3T	4899 ± 148	117 ± 7.8
J-21125.1	Dryer inlet manifold	HTO	88 970 ± 2670	2140 ± 140
J-21125.3		HT	66.6 ± 3.5	1.41 ± 0.1
J-21125.5		CH3T	<10	<0.2
J-21126.1	EDS outlet	HTO	18.3 ± 2.6	0.39 ± 0.1
J-21126.3		HT	<1 0	<0.2

the equivalent at sampling location 2. This is 529. The amount of HTO at sampling location 2 should be roughly equal to the sum of all total tritium activity at sampling location 1, but the actual value is ∼1/3 of this. It is concluded that the other 2/3 of HTO has been condensed and drained to the CRT, the condenser being located upstream of the sampling location 2.

6. Operating experience during TT and DT campaigns

6.1. Stack discharges

Weekly stack discharge data for HT and HTO is displayed in figure 32. Data is taken from the environmental compliance monitoring equipment. Emissions throughout the campaign remained within permitted discharge limits, with variations week by week of an order of magnitude for HT. HTO emissions typically follow a similar pattern with a few additional peaks.

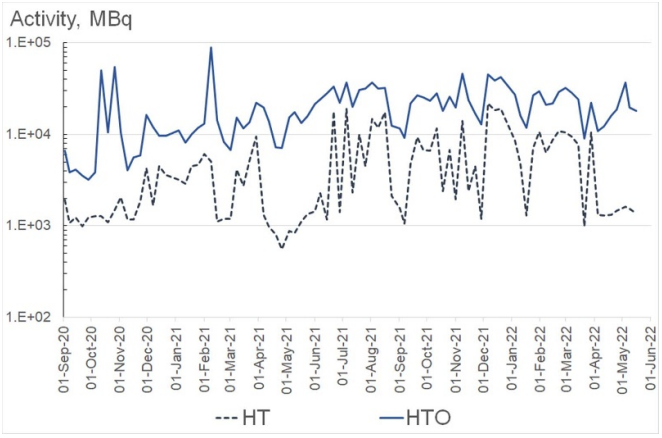

Figure 32. Weekly J25 stack discharges September 2020 on.

6.2. Dryer performance

During the operational phase, with very low flows of gas going to EDS and the system recycling a large portion of dry gas, the outlet humidity was around −100 °C dew point for extended periods of time, with dryers often in adsorption service for one month before being regenerated.

The dryer regenerations are shown in figure 33. Each dryer is represented, and quantities of water produced during each regeneration is shown. There is a gap from December 2020 to April 2022 during which time Dryer 1 was not used for adsorption. It is visible that initial quantities of water are higher than later in the operations. This is because during pre-tritium operations, dryers ran until saturation was detected; once dryers had some tritium into them, a rise in outlet IC was often seen before rise in outlet humidity, so dryers were changed over with outlet humidity remaining very low. From December 2020, Dryer 2 and 3 were routinely switched over every 2–4 weeks, pre-emptively to avoid reaching rising outlet IC or humidity conditions.

The activity of water captured in the dryers and sent to the ADT is in figure 34. To safely perform the analysis, the ADT samples required a 1000 000 times dilution. Two separate dilutions were performed on the sample taken on 14 January 2021,

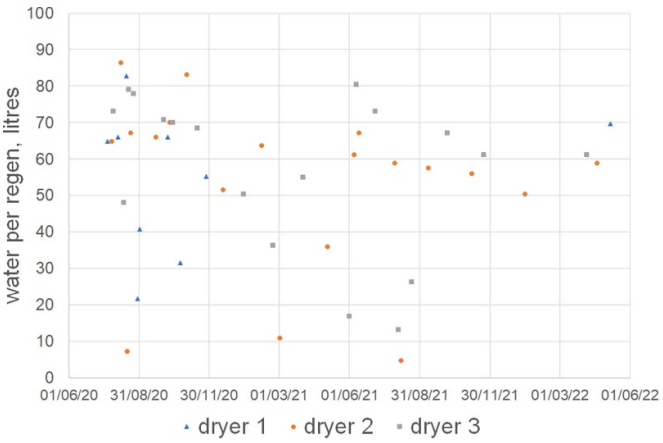

Figure 33. Dryer regenerations including quantities of water produced.

such a high dilution factor led to some uncertainty in the result. The total activity collected in the ADT is approximately 800 TBq.

6.3. Maintenance experience

Several breaches of EDS containment have been performed during active operations which are summarised: The gas side (downstream of recombiners) has been breached several times to replace the acid detector electrochemical cells. PPE

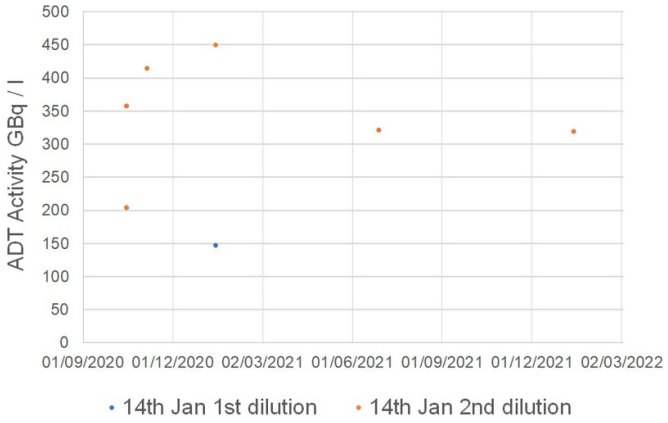

Figure 34. Active drain tank water activities.

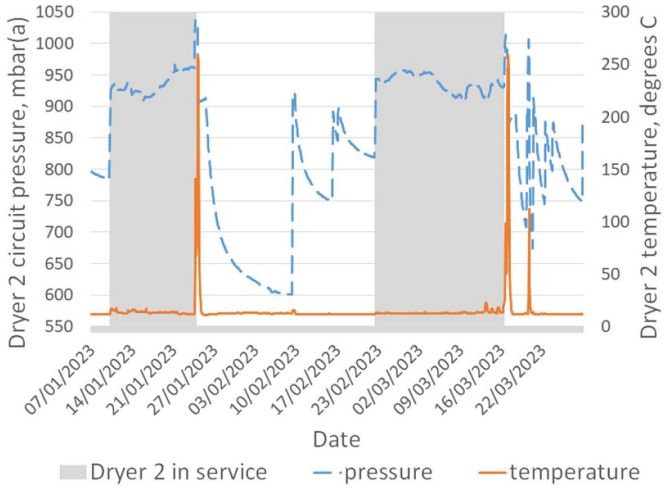

Figure 35. Dryer 2 pressure reduction following regenerations on 24 January 23 and 16 March 23.

consisted of coveralls and double gloves; LEV was in use at the location of the breach. During these breaches, no activity was observed from breathing zone tritium in air monitoring. The breaches were conducted when no potentially elevated sources of tritium were being discharged to EDS, but it demonstrates the low level of residual activity at this location.

Breaches on the wet side were conducted on 12 February 2021, to check and replace the condensate drain strainer filters. Due to the tritiated water hazard, operators wore plastic coveralls and boots and air fed hoods to minimise inhalation. With LEV in place throughout at the breach locations, tritium in air was between 7 MBq·m^{-3} (24 DAC—derived air concentration) and 11 MBq·m^{-3} (37 DAC), peaking at 17.5 MBq·m^{-3} (59 DAC) for $<$1 min. The increased airborne activity was also detected on the plant hall area monitor. The activity of water collected on molsieve dryers was significant and the Radiation Protection Advisor requested that any further breaches on the condensate lines/tank would require use of an isolator to ensure doses are ALARP. This experience and advice must be considered when designing and operating future tritiated water handling plant.

6.4. Operational issues

Some issues have been encountered during the operation of EDS which are described below.

6.4.1. Release of activity during dryer 1 regeneration. During regenerations of Dryer 1, activity was detected within the J25 casemate, a sealed room containing the CRT among other plant. As a precaution access to the area was restricted until confirmed safe by Health Physics survey.

No such issues have been detected during regeneration of Dryer 2 or 3. The activity was observed to increase as water drains from Dryer 1 condenser and collects into the tank, and to reduce when the CRT was subsequently drained to the ADT. It was decided to open the valve between the CRT and ADT during regeneration of Dryer 1 as a mitigation, which allowed water to flow from the condenser to the ADT without accumulation in the CRT.

Several investigations were performed to identify the leak path, involving fully draining down and isolating the tank and its drain lines, then pressurising with helium and searching the externals for traces of helium. No leak was identified. The decision was made to embargo use of Dryer 1 during the campaign operations pending further investigation. This meant operating with only two dryers, with safety analysis justifying the tolerable operational risk, that in the event of a duty dryer fault during regeneration of the other dryer, Dryer 1 could then be put into adsorption.

6.4.2. Dryer behaviour. Following dryer regenerations, dryer circuit pressure continues to reduce below atmospheric (and below the EDS operating pressure), even after the temperature has returned to ambient. This continues with the dryer in standby mode. The vacuum can be relieved by manually opening a valve which allows top up of gas from the dryer outlet manifold and another route allows this to happen automatically if the low pressure setpoint of a passive vacuum relief valve is reached. The probable cause is that the molsieve is absorbing residual water vapour from the closed loop, reducing the total gas pressure.

Figure 35 shows the Dryer 2 behaviour over two regeneration cycles. The post-regeneration temperature drops back to ambient relatively rapidly, hence this can be ruled out as the cause of the pressure reduction which occurs over a much longer period. The rapid recoveries in pressure occur on temporary opening of the vent valve. The rate of pressure reduction is observed to reduce over time. Unfortunately there is no humidity monitoring within the dryer circuit, however having ruled out temperature, there are no other credible causes of the pressure reduction other than that vapour adsorbing into the molsieve bed.

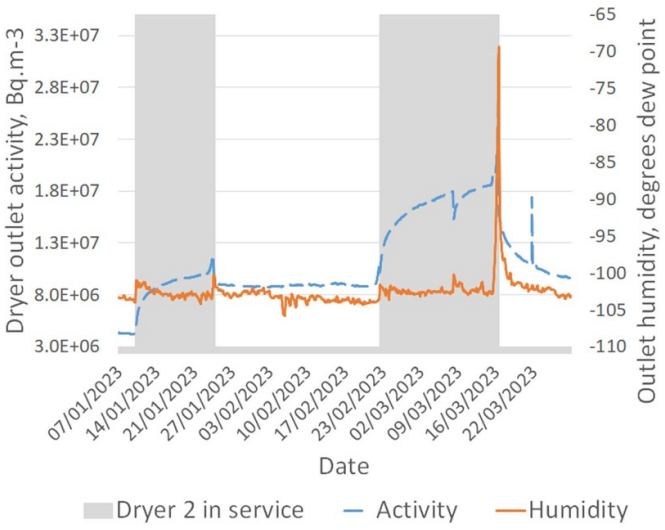

Figure 36. Outlet humidity and activity with dryer 2 and 3 alternating service.

On one occasion, dryer 3 blower automatically tripped when pressure fell below the setpoint. The dryer was vented as described above and blower restarted.

Figure 36 shows outlet humidity and tritium concentration for dryers 2 and 3. The saturation of the dryer is indicated by an increase in the humidity and/or the tritium concentration, either of these cases triggers the operator to start a new cycle of dryer changeover and regeneration.

Whilst Dryer 2 is in adsorption service, outlet activity is observed to rise slightly, and reduces once Dryer 2 is replaced by Dryer 3. Dryer 2 has received a higher loading of tritium during the campaign and the residual effect is still observed when it is put into adsorption duty.

6.4.3. Acid detector premature failures. Whilst testing with room air during the 6 months of EDS commissioning, the electrochemical cells performed as expected. However, once EDS was connected to JET and AGHS, the gas conditions were altered: during campaign operations EDS had very low flows of fresh gases, the bulk of gas being recirculated to maintain the nominal 180 $m^3 \cdot h^{-1}$ flowrate. Humidity at the dryer outlets in this regime typically sat around −100 °C DP, which is considerably lower than the 15% minimum relative humidity operating condition of the cells. The HF sensors consistently failed after only a few weeks service. This is put down to the extreme low humidity of the gas, drying out the electrolyte leading to premature failures. The manufacturer (Honeywell) has been contacted and confirmed the cells should not be operated outside of the humidities quoted in the datasheet. It was eventually decided to operate (after risk evaluation) with faulty HF sensors and replace them after the tritium campaign.

The operating mode resulting with low humidity was unfortunately not conceived during the gas detector design process. However, whilst a problem for EDS with its molecular sieve dryers and recycle, it is considered that detritiation systems operating with more humid conditions, such as those using wet scrubber columns, could successfully benefit from electrochemical cells for acid gas detection.

6.4.4. EDS availability. A few faults occurred which made EDS very briefly unavailable. All relate to electrical or control & instrumentation (EC&I) issues. The first occurred during a PLC communication repair. The second incident was a ProfiBus issue when a Siemens laptop was connected. The final time was due to Mains 2 power supply being lost: UPS 1 and 2 fault.

There have also been several occasions where recombiners have tripped on high temperature: due to thermocouple placement, some experience hotter conditions than others and are quite close to their trip limit. EDS would be deemed unavailable should the recombiners cool below a minimum threshold temperature, however in these instances the trips were reset and heater restarted in good time before the recombiner could cool down over the course of several hours.

6.5. Operational successes

Overall, the EDS performed well since going into service. The system has remained available throughout (with the exception of issues mentioned earlier). DF has been very high, the system has coped with a few discrete tritium ingress events, with no correlated rise in the outlet IC observed (but the dryer is then 'dirty', see section about elevated outlet IC following dryer changeover). Valve failures, which were an issue encountered on the original EDS [5] and have been cited as an argument against using interchangeable molsieve dryers for detritiation systems [6], have not occurred for this new system. The introduction of the novel passivation column has not led to any operational or performance issues, with measured pressure drops across the bed and outlet filter remaining stable throughout commissioning and operational phases.

6.5.1. Passivation system performance. There have been no instances of acid ingress, acute or chronic known to have occurred since operations began, so positive confirmation of acid neutralisation in service cannot be demonstrated.

At the end of non-active commissioning phase, the passivation filters were removed and replaced. Visual inspection of both the used filters and the top of the passivation bed was undertaken; no issues or degradation was observed at that point, the bed having been in service and exposed to a continuous flow of room air typically at 180 $m^3 \cdot h^{-1}$ for several months.

During tritium operations, the same passivation bed has remained in service throughout, and no notable increase in differential pressure across bed or outlet filter has been observed.

Based on the testing performed and operating experience gained since 2020, confidence in the Passivation System

remains high and the same technology (using high purity calcium hydroxide such as Loflosorb) is therefore recommended for any future detritiation systems where acid generation and damage is a risk.

7. Conclusion

The design and performance of the new JET EDS during commissioning and operations were presented. The original system was replaced due to pitting corrosion caused by halogenated acids which were produced in the high temperature recombiner. The new EDS design includes improvements compared to the original system to detect and mitigate against any further corrosion problems. Use of halogenated fluid and components must be avoided or controlled for fusion machines and fuel cycle plant.

During commissioning, the encountered issues (blower bearing failures, excessive water carry over during dryer regeneration, and vacuum relief valve failures) led to modifications to the plant and operating parameters to successfully resolve these issues. Commissioning tests effectively demonstrated the plant's DF (an order of magnitude higher than the 1000× requirement), recombiner operation and molsieve dryer performance.

During operations, the EDS has performed its duty, providing detritiation of exhaust gases, glovebox purge gas and air from LEV use. Dryer 1 was not used during the campaign following detection of a leak of tritium from the condensate drain, the leak location could not be pinpointed using helium and will be investigated again. Mobility of tritiated water vapour must be accounted for when designing and maintaining systems handling tritiated water.

The new passivation system performed well with high purity calcium hydroxide packing during bench testing and has not impacted EDS performance, therefore this solution is endorsed. HF gas detectors have failed prematurely due to very low humidity gas stream, resulting in frequent replacements, and are considered best suited to higher humidity systems.

A few modifications to EDS are planned for the future. A spray bar will be integrated into the condenser downstream of the passivation system to provide defence in depth should acid ingress re-occur, by washing/diluting any acid. A pH meter will be added to the CRT, adding further indication of any acidification of the condensate. Finally, demineralised water dosing pumps will be added to each dryer circuit. This isotopic swamping sub-system's purpose will be to promote molsieve bed detritiation by performing cycles of bed saturation with clean H_2O, followed by bed regeneration and collection in the ADT.

Data availability statement

The data cannot be made publicly available upon publication because no suitable repository exists for hosting data in this field of study. The data that support the findings of this study are available upon reasonable request from the authors.

Acknowledgments

This work has been carried out within the framework of the Contract for the Operation of the JET Facilities and has received funding from the European Union's Horizon 2020 research and innovation programme. The views and opinions expressed herein do not necessarily reflect those of the European Commission.

ORCID iD

Robert George https://orcid.org/0000-0003-2534-5219

References

[1] Rubel M 2019 Fusion neutrons: tritium breeding and impact on wall materials and components of diagnostic systems *J. Fusion Energy* **38** 315–29
[2] Gibney E 2022 Nuclear-fusion reactor smashes energy record *Nature* **602** 371
[3] Sabathier F, Brennan D, Skinner N and Patel B 2001 Assessment of the performance of the JET exhaust detritiation system *Fusion Eng. Des.* **54** 547–53
[4] Wong D P, Hemmerich J L and Monahan J J 1992 The exhaust detritiation system for the JET active gas handling plant—engineering, construction, installation and first commissioning results *Fusion Technol.* **21** 572–6
[5] Lässer R *et al* 1999 Use of the JET active gas handling plant exhaust detritiation system during and after DTE1 *Fusion Eng. Des.* **46** 307–12
[6] Perevezentsev A N, Andreev B M, Rozenkevich M, Pak Y S, Ovcharov A and Marunich S A 2010 Wet scrubber technology for tritium confinement at ITER *Fusion Eng. Des.* **85** 1206–10
[7] Glugla M 2014 Detritiation systems for ITER *Rayonnem. Ionis Tech. Mes. Prot.* **2014** 6–15
[8] Hemmerich J L, Bell A C, Boucquey P, Caldwell-Nichols C, Chuilon P, Delvart F 1993 *et al* Installation and inactive commissioning of the JET active gas handling system (AGHS) *15th IEEE/NPSS Symp. on Fusion Engineering-Supplement* (Abingdon: JET Joint Undertaking) pp 55–61
[9] UK Atomic Energy Authority 2018 Annual report and accounts 2017/18 *A History of Corporate Financial Reporting in Britain* (UK Atomic Energy Authority) (available at: https://assets.publishing.service.gov.uk/government/uploads/system/uploads/attachment_data/file/737294/UKAEA_annual_report___accounts_2017-18_-_web_version.pdf)
[10] Public Health England 2017 Hydrogen fluoride and hydrofluoric acid (HF) incident management (available at: https://assets.publishing.service.gov.uk/government/uploads/system/uploads/attachment_data/file/659083/Hydrogen_fluoride_incident_management.pdf)
[11] Nickel Institute 1976 Corrosion resistance of nickel-containing alloys in hydrofluoric acid, hydrogen fluoride and fluorine *INCO (Int Nickel Co, Inc.) Corros Man* (available at: https://nickelinstitute.org/media/4680/ni_inco_443_corrosionresisthydrofluoric.pdf)

[12] Budavari S 1996 *The Merck Index: An Encyclopedia of Chemicals, Drugs, and Biologicals* 12th edn (Whitehouse Station, NJ: Merck)
[13] Yao Y, Qiao L J and Volinsky A A 2011 Hydrogen effects on stainless steel passive film fracture studied by nanoindentation *Corros. Sci.* **53** 2679–83
[14] Yang Q, Qiao L J, Chiovelli S and Luo J L 1998 Effects of hydrogen on pitting susceptibility of type 310 stainless steel *Corrosion* **54** 628–33
[15] Ningshen S, Kamachi Mudali U, Amarendra G, Gopalan P, Dayal R K and Khatak H S 2006 Hydrogen effects on the passive film formation and pitting susceptibility of nitrogen containing type 316L stainless steels *Corros. Sci.* **48** 1106–21
[16] Bellanger G and Rameau J J 1995 Corrosion of nickel—chromium deposit on AISI 316L stainless steel in radioactive water with and without fluoride at pH 4 *J. Nucl. Mater.* **226** 104–19
[17] Fonseca A M, Órfão J J and Salcedo R L 1998 Kinetic modeling of the reaction of HCl and solid lime at low temperatures *Ind. Eng. Chem. Res.* **37** 4570–6